Infrared absorption of 3-propenonyl (CH2CHCO) radical generated upon photolysis of acryloyl chloride [CH2CHC(O)Cl] in solid para-H2

Prasanta Das and Yuan-Pern Lee

Citation: The Journal of Chemical Physics **139**, 084320 (2013); doi: 10.1063/1.4818880
View online: http://dx.doi.org/10.1063/1.4818880
View Table of Contents: http://scitation.aip.org/content/aip/journal/jcp/139/8?ver=pdfcov
Published by the AIP Publishing

Infrared absorption of 3-propenonyl (·CH_2CHCO) radical generated upon photolysis of acryloyl chloride [$CH_2CHC(O)Cl$] in solid *para*-H_2

Prasanta Das[1] and Yuan-Pern Lee[1,2,a)]
[1]*Department of Applied Chemistry and Institute of Molecular Science, National Chiao Tung University, Hsinchu 30010, Taiwan*
[2]*Institute of Atomic and Molecular Sciences, Academia Sinica, Taipei 10617, Taiwan*

(Received 13 June 2013; accepted 6 August 2013; published online 29 August 2013)

Irradiation at 193 nm of a *p*-H_2 matrix containing acryloyl chloride $CH_2CHC(O)Cl$ at 3.2 K yielded infrared absorption lines at 3143.6 (ν_1), 3057.0 (ν_2), 3048.0 (ν_3), 2103.1 (ν_4), 1461.0 (ν_5), 1349.8 (ν_6), 1223.7 ($\nu_{11}+\nu_{12}$ or $2\nu_{12}$), 1092.8 (ν_8), 918.1 (ν_9), 691.0 (ν_{10}), 624.3 (ν_{11}), and 597.1 (ν_{12}) cm^{-1} that are assigned to the 3-propenonyl (·CH_2CHCO) radical. The assignments are based on the photolytic behavior and a comparison of observed vibrational wavenumbers and infrared intensities with those predicted with the B3PW91/aug-cc-pVDZ method. The observation is consistent with a major radical formation channel CH_2CHCO + Cl followed by escape of the Cl atom from the original *p*-H_2 cage. The observation of 3-propenonyl (·CH_2CHCO) radical but not 3-propenalyl (*s-cis*- or *s-trans*-$CH_2C\dot{H}CO$) radical indicates that the former is the most stable isomer and that the barrier heights for conversion from *s-cis*- or *s-trans*-$CH_2C\dot{H}CO$ to ·CH_2CHCO are small.
 [http://dx.doi.org/10.1063/1.4818880]

I. INTRODUCTION

Acryloyl chloride ($CH_2CHC(O)Cl$, also known as propenoyl chloride, acrylyl chloride, or acrylic acid chloride) is a simple α,β-unsaturated chlorocarbonyl compound. Because of the presence of the enone (C=C−C=O) functional group, acryloyl chloride exhibits rich photochemistry with various photolytic paths. It serves as an important building block for further functionalization and an excellent substrate for cross-metathesis in various polymerization, biological, and medical applications.[1–4] The fission of the C−Cl bond of $CH_2CHC(O)Cl$ produces Cl atom and C_2H_3CO radical, a crucial intermediate that has been proposed in reactions between O atom and propargyl (C_3H_3) radical in combustion and atmospheric chemistry.[5]

Extensive experimental investigations on $CH_2CHC(O)Cl$ have been conducted. These include structural and spectral studies,[6–11] pyrolysis,[12] photolysis,[13–18] and photoionization.[19] Quantum-chemical calculations were also performed to predict the enthalpy, vibrational frequencies, electronic states, and reaction paths for isomerization and dissociation of $CH_2CHC(O)Cl$.[10,15,17,19,20]

Szpunar *et al*. employed photofragment translational spectroscopy to investigate the primary and secondary dissociation channels of $CH_2CHC(O)Cl$ excited at 193 nm.[15] They observed two C−Cl fission channels that produced C_2H_3CO with large and small kinetic energies, respectively, but the C_2H_3CO radicals produced in both channels had sufficient internal energy to undergo secondary decomposition so that only products C_2H_3 + CO were detected. Lau *et al*. excited $CH_2CHC(O)Cl$ at 235 nm, at which most C_2H_3CO fragment is stable, and employed two-dimensional product-velocity-map imaging to determine the barrier height for the decomposition of C_2H_3CO to C_2H_3 + CO to be ∼92 kJ mol^{-1}.[16] Because of the similarity in energy, they employed wavelength 157 nm to photoionize all isomeric C_2H_3CO fragments formed on photodissociation of $CH_2CHC(O)Cl$ at 235 nm; no information about the conformation of the C_2H_3CO fragments was available.

Three conformers of C_2H_3CO were predicted to be stable: *s-cis*- and *s-trans*-3-propenalyl radicals (also known as prop-2-en-1-one, 1-oxo-2-propenyl, propenyloxy, or propenoyl, designated $CH_2C\dot{H}CO$ in this paper) with the carbonyl group *cis*- and *trans*- with respect to the CH_2 group, respectively, and 3-propenonyl (also known as prop-2-en-3-one or 3-oxo-2-propenyl, designated ·CH_2CHCO in this paper) with a nearly linear CCO group,[21] as shown in Fig. 1. In this paper we indicate this radical as C_2H_3CO when the conformation is unspecified. Early calculations using various methods including CCSD(T)//QCISD/6-311G(d,p) predicted that *s-trans*-$CH_2C\dot{H}CO$ is the most stable conformer,[21] but recent calculations using CCSD(T)/aug-cc-pV(Q+d)Z//CCSD(T)/6-311G(2df,p) and the G3 methods predicted that ·CH_2CHCO is the most stable and that the energy differences among these three conformers are within 8 kJ mol^{-1}.[16] The potential-energy curves along the torsional coordinate to transform between these three conformers were predicted to be nearly flat, with barriers less than 11 kJ mol^{-1}.[21]

No spectral information on gaseous C_2H_3CO in any conformation has been reported. Baskir and Nefedov observed characteristic IR features of $CH_2C\dot{H}CO$ isolated in solid Ar at 1823.1 and 1832.0 cm^{-1} along with some weak lines at 1094.4, 975.3, and 870.7 cm^{-1} upon photolysis of allylperoxy

a)Author to whom correspondence should be addressed. Electronic mail: yplee@mail.nctu.edu.tw.

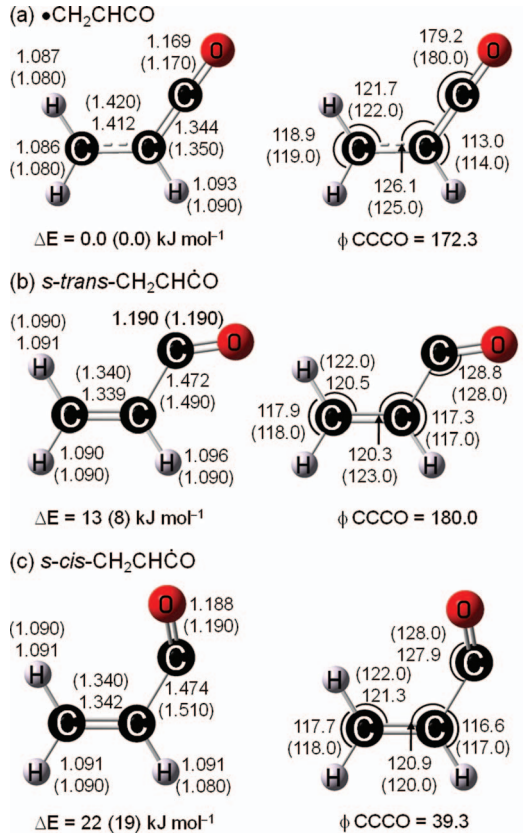

FIG. 1. Geometries and relative energies (in kJ mol^{-1}, corrected for zero-point energy) of (a) ·CH_2CHCO (3-propenonyl), (b) *s-trans*-CH_2CHCO (*3*-propenalyl), and (c) *s-cis*-CH_2CHCO predicted with the B3PW91/aug-cc-pVDZ method. Bond distances are in Å and angles are in degrees. Parameters predicted with the QCISD/6-311G(d,p) method and energies obtained with the B3LYP/6-311G(d,p) method are listed in parenthesis.[21]

radical, $H_2C = CHCH_2OO$, which was produced upon pyrolysis of 1,5-hexadiene, followed by reaction with O_2 during deposition.[22] Pietri *et al*. used light of wavelength ≥310 nm from a high-pressure Hg lamp to photolyze $CH_2CHC(O)Cl$ isolated in an Ar matrix at 10 K and observed IR absorption of only 3-chloro-1,2-propenone, $CH_2ClCHCO$, with a characteristic broad feature near 2139 cm^{-1}; they ascribed the mechanism of formation to involve 1,3-chlorine migration, and reported no absorption ascribable to CH_2CHCO.[14] The formation of only $CH_2ClCHCO$ in this experiment might be due to the matrix cage effect;[14] upon C−Cl fission, the Cl fragment cannot escape from the original cage so the secondary reaction of Cl + C_2H_3CO yields $CH_2ClCHCO$. Cui *et al*. undertook various quantum-chemical calculations to map the potential-energy surfaces of isomerization and dissociation reactions of $CH_2CHC(O)Cl$ in its S_0, T_1, T_2, and S_1 states.[20] They indicated that, upon photoexcitation at 310 nm, $S_1 \rightarrow T_1$ intersystem crossing is the dominant primary process, which is followed by 1,3-Cl migration along the T_1 path, whereas, for excitation at a wavelength smaller than 230 nm, C−Cl bond cleavage is the exclusive primary channel.

Wu *et al*. employed time-resolved Fourier-transform infrared (FTIR) absorption spectroscopy to detect the photolysis products of $CH_2CHC(O)Cl$ in solution upon excitation at 193 or 266 nm.[17] They ascribed the intense feature near 2128 cm^{-1} with a life time ∼280 μs to $CH_2ClCHCO$ and a weak line near 1813 cm^{-1} to CH_2CHCO that decays within a few μs; the former was produced from a stepwise mechanism involving dissociation and recombination. The reason that the most stable conformer ·CH_2CHCO predicted by quantum-chemical calculations is observed neither in a low-temperature inert-gas matrix nor in a solution remains to be explained.

The quantum solid *para*-hydrogen (*p*-H_2) has a diminished cage effect that allows the production of free radicals via photofragmentation[23–25] *in situ* or bimolecular reactions induced on irradiation.[26–30] In this work, we have photolyzed a $CH_2CHC(O)Cl$/*p*-H_2 matrix at 3.2 K with laser light at 193 nm and observed absorption lines ascribable to 11 fundamental vibrational modes of 3-propenonyl (·CH_2CHCO) radical.

II. EXPERIMENTS

As the apparatus and experimental procedures for IR absorption spectra of *p*-H_2 matrix-isolation are similar to those discussed previously, only a brief description is given.[26,30] A gold-plated copper block was attached to a closed-cycle refrigerator system and cooled to 3.2 K. It served as both a matrix sample substrate and a reflector of the incident IR beam to the detector. A gaseous mixture of $CH_2CHC(O)Cl$/*p*-H_2 (1/2500–1/3000) was typically deposited at flow rate of ∼14 mmol h^{-1} over a period of 9 h. IR absorption spectra at resolution 0.25 cm^{-1} were recorded with a FTIR spectrometer, equipped with a KBr beam splitter and a HgCdTe detector cooled to 77 K; 900 scans were typically averaged after each stage of experiments. The IR beam of the spectrometer was passed through a filter (2.4 μm cutoff) to block light of wavenumber greater than 4000 cm^{-1} to avoid the reaction of Cl atoms with vibrationally excited H_2 produced upon absorption of the unfiltered IR light.[31]

We employed light at 295 nm and 193 nm for photolysis of matrix samples in separate experiments. The 532-nm output (280 mJ pulse^{-1}) of a pulsed Nd:YAG laser (Spectra Physics, GCR5, 10 Hz) was used to pump a dye laser (Sirah, Precision Scan) containing a dye solution of sulforhodamine B in methanol to generate visible radiation in the region 585–600 nm. The dye output was then frequency-doubled with a potassium dihydrogen phosphate (KDP) crystal to yield light at 295 nm with energy 5–7 mJ pulse^{-1}. An ArF excimer laser (Coherent, COMPexPro-50), operated at 10 Hz with energy 3–5 mJ pulse^{-1}, provided radiation at 193 nm. The light source for secondary photolysis was a KrF excimer laser (248 nm, Lambda Physik, LPX200) operated at 1 Hz with energy 5–8 mJ pulse^{-1}.

The mixing ratios of the precursor and observed photolysis products were estimated according to the expression,[32]

$$c\,(\text{in ppm}) = \frac{2.303 \int \log_{10}(I/I_0)dv}{\varepsilon l} V_0 \times 10^6,$$

in which the numerator is the integrated line intensity (in cm^{-1}), ε (in cm mol^{-1}) is the absorption coefficient, *l* (in cm)

is the optical path length through the *p*-H_2 matrix measured according to the procedure described by Tam *et al.*,[33] and $V_0 = 23.16$ cm^3 mol^{-1} is the molar volume of solid *p*-H_2.[34] Experimental absorption coefficients were used for CO,[32] C_2H_2,[35] C_2H_4,[36] and HCl,[37] whereas IR intensities calculated with the B3PW91/aug-cc-pVDZ method were used for $C_2H_3C(O)Cl$, CH_2CHCO, C_2H_5, CH_2CCO, $CH_2ClCHCO$, C_2H_3Cl, and ClCO. Typical values of l are ∼0.2 cm after 9 h deposition with a flow rate of ∼14 mmol h^{-1}. Typically we chose 2–4 absorption lines of one species and averaged the derived mixing ratios; the fitting errors are typically within ±20%, but in cases when only quantum-chemically predicted IR intensities were available the error might be greater.

As acryloyl chloride (96%, Aldrich, containing ∼400 ppm phenothiazine stabilizer) undergoes slow polymerization at room temperature, we applied the freeze-pump-thaw method to remove the impurities before preparation of a sample mixture. The mixing ratio of *o*-H_2 is estimated to be less than 100 ppm when we cooled the hydrous iron (III) oxide catalyst to ∼12 K.

III. COMPUTATIONS

The geometries, harmonic and anharmonic vibrational wavenumbers, and IR intensities of *s-cis*/*s-trans* conformers of $CH_2CHC(O)Cl$, $CH_2ClCHCO$, and three conformers of C_2H_3CO radicals were calculated with the B3PW91 density-functional theory[38,39] using Dunning's correlation-consistent polarized-valence double-zeta basis set, augmented with *s*, *p*, *d*, and *f* functions (aug-cc-pVDZ).[40] Vibrational wavenumbers were calculated analytically at each stationary point. The anharmonic effects were calculated with a second-order perturbation approach using an effective finite-difference evaluation of the third and semidiagonal fourth derivatives. All theoretical calculations were conducted with the GAUSSIAN 09 program.[41]

A. *s-cis*- and *s-trans*-$CH_2CHC(O)Cl$ and $CH_2ClCHC{=}O$

The structural parameters of *s-trans*- and *s-cis*-$CH_2CHC(O)Cl$ and $CH_2ClCHCO$ optimized with the B3PW91/aug-cc-pVDZ method are shown in Figs. S1(a)–S1(c) in the supplementary material;[42] those previously measured with the electron diffraction method for *s-cis*- and *s-trans*-$CH_2CHC(O)Cl$ conformers[8] and those predicted with the MP2/6-31G* method for $CH_2ClCHCO$ are listed parenthetically.[14] According to the B3PW91/aug-cc-pVDZ and B3PW91/aug-cc-pVQZ methods, *s-trans*-$CH_2CHC(O)Cl$ is more stable than *s-cis*-$CH_2CHC(O)Cl$ by 0.4 and 0.1 kJ mol^{-1}, respectively. Considering the errors in theoretical predictions, we conclude that both isomers are close in energy, consistent with a value of only ∼1.0 kJ mol^{-1} determined with gas-phase electron diffraction at varied temperature for the energy of *s-cis*-$CH_2CHC(O)Cl$ relative to that of *s-trans*-$CH_2CHC(O)Cl$.[8] The energy of $CH_2ClCHCO$ is predicted to be 39 kJ mol^{-1} greater than that of *s-trans*-$CH_2CHC(O)Cl$, slightly smaller than the reported value 43 kJ mol^{-1} obtained with the MP2/6-31G* method.

At the B3PW91/aug-cc-pVDZ level of theory, the anharmonic (harmonic) vibrational wavenumbers for IR absorption lines of *s-trans*- and *s-cis*-$CH_2CHC(O)Cl$ with intensities greater than 30 km mol^{-1} are 1806 (1842), 1381 (1418), 1137 (1161), 990 (1022), 983 (1006), and 601 (605) cm^{-1} and 1817 (1853), 1636 (1677), 1380 (1415), 970 (988), and 704 (709) cm^{-1}, respectively. The anharmonic vibrational wavenumbers and relative IR intensities of some representative modes for both conformers are presented in Table I. A comparison of harmonic and anharmonic vibrational wavenumbers of both conformers is available in Table SI.[42]

Harmonic and anharmonic vibrational wavenumbers and relative IR intensities of $CH_2ClCHCO$ predicted with the B3PW91/aug-cc-pVDZ method are listed in Table II. The C=O stretching mode at 2184 (2222) cm^{-1} is the most prominent, with weaker modes having IR intensities greater than 20 km mol^{-1} at 1231 (1253), 1003 (1037), 668 (686), and 548 (556) cm^{-1}.

B. ·CH_2CHCO and *s-cis*/*s-trans*-$CH_2C\dot{H}CO$ radicals

The C_2H_3CO radical has three stable conformers: *s-cis* and *s-trans* form of 3-propenalyl ($CH_2C\dot{H}CO$) with the unpaired electron located on the carbonyl carbon atom and 3-propenonyl (·CH_2CHCO) with the unpaired electron located mainly on the terminal carbon atom. The geometries of these conformers computed with the B3PW91/aug-cc-pVDZ method are shown in Figs. 1(a)–1(c). The structural parameters previously predicted with the QCISD/6-311G(d,p) method are listed in parentheses for comparison.[21] The structures of these isomers are consistent with the previously reported structures, except that Cooksy[21] reported that *s-cis*-3-propenalyl is planar, whereas our calculations indicate that C=O group bends from the CH_2CH molecular plane by ∼40°. The most stable structure among these isomers is the ·CH_2CHCO radical, which has a linear C=C=O structure. The energies of the s-*trans*- and *s-cis*-$CH_2C\dot{H}CO$ radicals relative to ·CH_2CHCO are 13 and 22 kJ mol^{-1}, respectively, slightly larger than the values of 8 and 19 kJ mol^{-1} calculated with the B3LYP/6-311G* method.[21] The experimental enthalpies of formation ΔH_f^0 of ·CH_2CHCO and *s-cis*/*s-trans*-$CH_2C\dot{H}CO$ radicals are unreported; we evaluated $\Delta H_f^0 = -131$, -109, and -118 kJ mol^{-1} for these three conformers at 298 K, respectively.

The harmonic and anharmonic vibrational wavenumbers and relative IR intensities predicted with the B3PW91/aug-cc-pVDZ method for ·CH_2CHCO and *s-cis*/*s-trans*-$CH_2C\dot{H}CO$ are listed in Table II. The anharmonic (harmonic) vibrational modes of ·CH_2CHCO with IR intensities greater than 8 km mol^{-1} are predicted at 3019 (3179), 2139 (2184), 674 (710), and 605 (578) cm^{-1}; the intensity (634 km mol^{-1}) of the C=O stretching mode at 2139 cm^{-1} is at least 14 times as great as that of another line. In contrast, the most intense C=O stretching modes in *s-cis*- and *s-trans*-$CH_2C\dot{H}CO$ are predicted to be near 1881 and 1870 cm^{-1}, with IR intensities 182 and 245 km mol^{-1}, respectively, and lines near 955, 946, and 691 cm^{-1} for

TABLE I. Comparison of experimental vibrational wavenumbers (cm^{-1}) and relative IR intensities of *s-cis*- and *s-trans*-$CH_2CHC(O)Cl$ with anharmonic vibrational wavenumbers and relative IR intensities predicted with the B3PW91/aug-cc-pVDZ method.

		p-H_2 (cm^{-1} (%))		Gas phase (cm^{-1})		Ar-matrix (cm^{-1})		B3PW91/aug-cc-pVDZ	
Mode	Sym	*s-trans*	*s-cis*	*s-trans*	*s-cis*	*s-trans*	*s-cis*	*s-trans*	*s-cis*
ν_1	A′	3118.4 (0.7)[a]		3122				3119 (0.1)[a]	3123 (0.0)[a]
ν_2	A′	3039.9 (0.7)		3069	3087			3059 (0.3)	3100 (0.2)
ν_3	A′	2993.1 (0.2)	3034.8 (0.8)[a]	3043				2991 (0.5)	3054 (0.8)
ν_4	A′	1768.2 (100)	1779.6 (80)	1789[b]	1775[b]	1766	1779	1806 (100)	1817 (87)
ν_5	A′	1625.9 (2.1)	1616.7 (8.5)	1628	1620	1626	1619	1656 (1.2)	1636 (14)
ν_6	A′	1395.6 (31)[c]	1395.6 (31)[c]	1397		1394	1398	1381 (8.5)	1380 (22)
ν_7	A′	1284.0 (1.1)	1287.5 (0.4)	1285		1284	1288	1275 (0.4)	1279 (1.2)
ν_8	A′	1149.9 (53)	1074.0 (2.1)	1152		1150	1075	1137 (40)	1069 (5.3)
ν_9	A′	937.9 (63)	976.3 (100)	939	979	936	973	932 (26)	970 (100)
ν_{10}	A′	607.1 (39)	708.1 (37)	609	708	605	705	601 (21)	704 (34)
ν_{11}	A′	494.8 (16)		494[d]	446	494	446	488 (6.7)	439 (7.0)
ν_{12}	A′			445	386			430 (4.3)	383 (6.2)
ν_{13}	A′			257				256 (0.0)	252 (0.4)
ν_{14}	A″		982.7 (13)	981[d]	983	984	999	990 (5.1)	992 (11)
ν_{15}	A″			977[d]	975	979[b]	986[b]	983 (9.2)	976 (5.7)
ν_{16}	A″	756.5 (7.6)	743.2 (5.1)	757	744	756	744	759 (3.6)	746 (5.2)
ν_{17}	A″			452[d]	485			442 (0.0)	473 (0.0)
ν_{18}	A″			108	95			110 (0.2)	73 (0.0)
Reference		This work	This work	9	9	14	14	This work	This work

[a]Percentage IR intensities relative to the most intense line are presented in parentheses. IR intensities of these most intense lines are predicted to be 350 (1806 cm^{-1}) and 288 km mol^{-1} (970 cm^{-1}) for *s-trans*- and *s-cis*-$CH_2CHC(O)Cl$, respectively.
[b]Assignments might have to be switched between these two conformers according to theoretical calculations.
[c]Total intensity of these two overlapped lines.
[d]Assignments of these two modes are switched from the original report according to theoretical calculations.

TABLE II. Comparison of observed vibrational wavenumbers (in cm^{-1}) and relative IR intensities of $\cdot CH_2CHCO$ with anharmonic vibrational wavenumbers and relative IR intensities of $\cdot CH_2CHCO$, $CH_2CH\dot{C}O$ (*s-cis* and *s-trans*), $CH_2ClCHCO$, and CH_2CCO predicted with the B3PW91/aug-cc-pVDZ method and experimental data of CH_2CCO.

	p-H_2	B3PW91/aug-cc-pVDZ					Ar[a]
Mode	$\cdot CH_2CHCO$ cm^{-1} (%)	$\cdot CH_2CHCO$ cm^{-1} (%)	*s-cis*-$CH_2CH\dot{C}O$ cm^{-1} (%)	*s-trans*-$CH_2CH\dot{C}O$ cm^{-1} (%)	$CH_2ClCHCO$ cm^{-1} (%)	CH_2CCO cm^{-1} (%)	CH_2CCO cm^{-1}
ν_1	3143.6 (0.3)[b]	3139 (0.3)[b]	3111 (1.1)[b]	3105 (0.6)[b]	3067 (1.3)[b]	3014 (0.6)[b]	3049/3024
ν_2	3057.0 (0.5)	3046 (0.4)	3039 (0.6)	3015 (1.5)	3025 (0.2)	2944 (3.0)	2978/2974
ν_3	3048.0 (1.2)	3019 (1.4)	3004 (0.7)	2956 (4.1)	2978 (1.0)		
ν_4	2103.1 (100)	2139 (100)	1881 (100)	1870 (100)	2184 (100)	2187 (100)	2125
ν_5	1461.0 (0.1)	1442 (0.2)	1552 (2.7)	1638 (0.9)	1419 (1.4)	1742 (1.0)	1690
ν_6	1349.8 (0.3)	1348 (0.2)	1369 (4.2)	1370 (8.0)	1394 (1.8)	1433 (0.1)	1444
...[c]	1223.7 (0.7)	1235					
ν_7		1167 (1.0)	1263 (0.8)	1251 (0.1)	1231 (6.1)	1040 (2.1)	1046
ν_8	1092.8 (0.4)	1080 (0.9)	1050 (1.7)	1075 (10)	1159 (2.5)	1000 (2.5)	980
ν_9	918.1 (0.4)	908 (0.4)	955 (27)	988 (13)	1124 (0.0)	911 (0.3)	903
ν_{10}	691.0 (4.7)	674 (6.4)	946 (8.9)	962 (8.5)	1003 (3.2)	676 (1.1)	668
ν_{11}	624.3 (0.4)	630 (0.4)	835 (2.6)	870 (4.8)	859 (1.3)		
ν_{12}	597.1 (6.5)	605 (7.1)	691 (7.5)	600 (1.7)	668 (16)		
ν_{13}		390 (2.1)	437 (3.2)	527 (2.4)	630 (1.2)	474 (1.2)	473
ν_{14}		294 (0.1)	246 (4.6)	320 (0.6)	548 (2.9)	260 (0.2)	
ν_{15}		212 (0.4)	147 (1.6)	143 (0.0)	521 (0.1)[d]	156 (2.3)	

[a]From Ref. 47. Additional lines at 2603 ($2\nu_8 + \nu_{10}$), 2177 ($\nu_5 + \nu_{13}$), 2079 ($2\nu_7$), and 1959 ($2\nu_8$) cm^{-1} were reported with our tentative assignments given in parentheses.
[b]Percentage relative IR intensities to the most intense line are listed in parenthesis. IR intensities of these lines are 634, 182, 245, 842, and 973 km mol^{-1} for $\cdot CH_2CHCO$, *s-cis*-$CH_2CH\dot{C}O$, *s-trans*-$CH_2CH\dot{C}O$, $CH_2ClCHCO$, and CH_2CCO, respectively.
[c]Tentatively assigned to $\nu_{11} + \nu_{12}$ and/or $2\nu_{12}$.
[d]Additional modes of $CH_2ClCHCO$ are predicted to have anharmonic vibrational wavenumbers (relative IR intensities): 301(2.4), 200 (0.1), 73 (0.2).

s-cis- $CH_2CH\dot{C}O$ and those near 1370, 988, and 962 cm^{-1} for *s-trans*-$CH_2CH\dot{C}O$ have intensities greater than 7% of that of the most intense feature.

C. CH_2CCO

Propadienone, CH_2CCO, might be produced from $CH_2CHC(O)Cl$ via elimination of HCl. An analysis of microwave spectra for the vibrational ground state indicates that the equilibrium structure of propadienone belongs to point group C_s with the C=C=O moiety slightly nonlinear.[43,44] as shown in Fig. S2 of the supplementary material;[42] the structural parameters of CH_2CCO optimized with the B3PW91/aug-cc-pVDZ method are also shown for comparison. The anharmonic vibrational wavenumbers and IR intensities for CH_2CCO calculated with the B3PW91/aug-cc-pVDZ method are listed in Table II. The anharmonic (harmonic) vibrational modes of CH_2CCO with IR intensities greater than 20 km mol^{-1} are predicted at 2944 (3096), 2187 (2227), 1040 (1059), 1000 (1027), and 156 (171) cm^{-1}, with the line at 2187 cm^{-1} being the most intense (973 km mol^{-1}) and other lines at most 1.2% that intensity.

IV. EXPERIMENTAL RESULTS

A. $CH_2CHC(O)Cl/p\text{-}H_2$ matrices

The IR spectrum of a sample of $CH_2CHC(O)Cl/p\text{-}H_2$ (1/3000) at 3.2 K is shown in Fig. 2(a). Lines observed in two sets at 3034.8, 1779.6, 1616.7, 1395.6, 1287.5, 1074.0, 982.7, 976.3, 743.2, and 708.1 cm^{-1} and at 3118.4, 3039.9, 2993.1, 1768.2, 1625.9, 1395.6, 1284.0, 1149.9, 937.9, 756.5, 607.1, and 494.8 cm^{-1} are assigned to *s-cis* and *s-trans* conformers of $CH_2CHC(O)Cl$, and marked as "*c*" and "*t*," respectively. Piétri *et al*. observed partial conversion of *s-trans*-$CH_2CHC(O)Cl$ to *s-cis*-$CH_2CHC(O)Cl$ upon irradiation of the $CH_2CHC(O)Cl$/Ar matrix sample with light of $\lambda > 310$ nm.[14] We irradiated the matrix sample at 295 nm and also found that the *s-trans* conformer was converted to the *s-cis*-conformer. A difference spectrum obtained on subtracting the spectrum of a $CH_2CHC(O)Cl/p\text{-}H_2$ matrix recorded upon deposition [Fig. S3(a)] from that recorded after irradiation with light at 295 nm for 2 h is presented in Fig. S3(b) of the supplementary material;[42] lines due to *s-cis*- and *s-trans*-conformers are clearly distinguished as they are pointing upwards and downwards, respectively. Observed vibrational wavenumbers are compared with the predicted values and reported experimental values in the gaseous phase[9] and in an Ar-matrix[14] in Table I. The original assignments of ν_{11} and ν_{17} for *s-trans*-$CH_2CHC(O)Cl$ are interchanged according to theoretical calculations. We estimated the mixing ratios of *s-cis*-$CH_2CHC(O)Cl$ and *s-trans*-$CH_2CHC(O)Cl$ to be approximately (78 ± 14) and (150 ± 10) ppm according to Fig. S3(a); assuming a Boltzmann distribution at 298 K, the ratio of 0.52 ± 0.14 corresponds to an energy difference of 1.6 ± 0.7 kJ mol^{-1}, slightly greater than the reported value of 1.0 kJ mol^{-1} determined from electron diffraction,[8] but within experimental uncertainties. After irradiation of the matrix sample at 295 nm for 2 h, the mixing ratios were found to be approximately (103 ± 16) and (84 ± 4) ppm for *s-cis* and *s-trans* conformers, respectively, according to Fig. S3(b),[42] indicating that some $CH_2CHC(O)Cl$ was photolyzed at this wavelength.

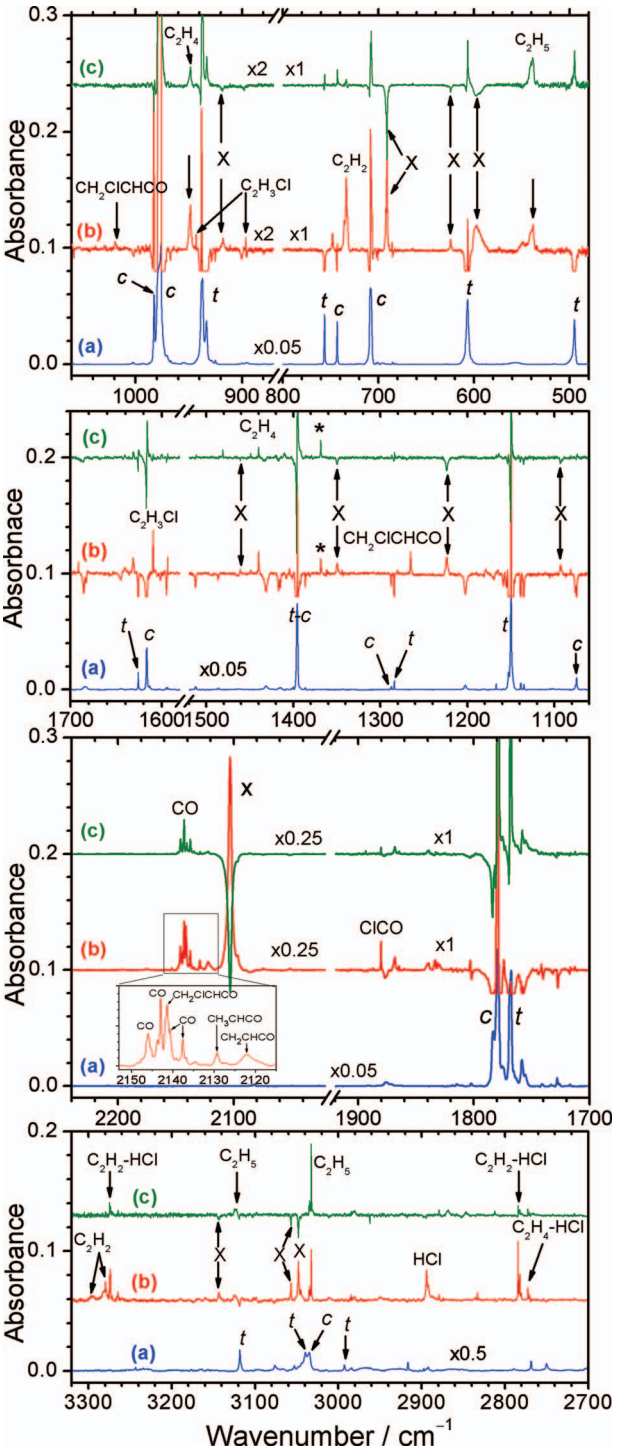

FIG. 2. (a) Absorption spectrum of a $CH_2CHC(O)Cl/p\text{-}H_2$ (1/3000) matrix deposited at 3.2 K for 9 h. (b) Difference spectrum of this matrix upon irradiation with light at 193 nm for 70 min. (c) Difference spectrum of this matrix after further photolysis with 248 nm for 10 min. All experimental spectra were recorded at resolution 0.25 cm^{-1}. Lines marked with "*c*" and "*t*" in trace (a) are assigned to *s-cis*- and *s-trans*-$CH_2CHC(O)Cl$, respectively. Lines in group X (·CH_2CHCO) are indicated with arrows in traces (b) and (c). Prominent lines of C_2H_2, C_2H_2-HCl, C_2H_4, C_2H_4-HCl, C_2H_5, C_2H_3Cl, $CH_2ClCHCO$, CH_3CHCO, and CH_2CCO are also indicated.

B. Photolysis of $CH_2CHC(O)Cl/p\text{-}H_2$ matrices at 193 nm

When the $CH_2CHC(O)Cl/p\text{-}H_2$ (1/3000) matrix sample at 3.2 K was irradiated with light at 193 nm, lines due to *s-cis*- and *s-trans*-$CH_2CHC(O)Cl$ decreased and new IR features in several groups appeared. A difference spectrum obtained on subtracting the spectrum recorded upon deposition from that recorded upon irradiation for 70 min is presented in Fig. 2(b); lines pointing upwards indicate production, whereas the most intense parts of the downward lines due to destruction of the precursor are truncated. We performed secondary photolysis with several light sources to distinguish lines from various carriers. For comparison, we present in Fig. 2(c) a difference spectrum obtained on subtracting the spectrum in Fig. 2(b) from that recorded upon secondary photolysis at 248 nm for 10 min.

These new features in Fig. 2(b) are separated into several groups. Intense lines observed near 2145.9, 2142.9, 2140.6, and 2137.6 cm^{-1} are assigned to CO; these line positions are similar to those reported for rotational lines of CO isolated in $p\text{-}H_2$.[45] Lines of groups A, B, and C, listed in Table III, are readily assigned to C_2H_2, C_2H_4, and C_2H_5, according to literature reports; they are directly marked as "C_2H_2," "C_2H_4," and "C_2H_5" in Fig. 2(b), respectively. The intensities of lines at 3294.9, 3279.6, and 733.7 cm^{-1} (group A, assigned to C_2H_2)[46] attained maxima after photolysis at 193 nm for 15 min, but remained nearly unchanged when the matrix was subsequently irradiated with light at 248 nm. The intensity of features of C_2H_4 (group B)[46] at 1440.0 and 948.6 cm^{-1} increased gradually when the matrix was irradiated further at 193 nm or with light at 248 nm for 10 min. The intensities of lines observed at 3124.8, 3032.6, and 538.5 cm^{-1} (group C, assigned to C_2H_5)[46] increased significantly at the initial stage of irradiation at 193 nm and increased further upon secondary photolysis at 248 nm for 10 min.

Lines at 3143.6, 3057.0, 3048.0, 2103.1, 1461.0, 1349.8, 1223.7, 1092.8, 918.1, 691.0, 624.3, and 597.1 cm^{-1} appeared upon photolysis at 193 nm but their intensities decreased upon secondary photolysis at 248 nm. These lines, denoted as group X and indicated with "X" in Fig. 2, match no known absorption lines of possible products. They are assigned to 3-propenonyl ($\cdot CH_2CHCO$) radical, to be discussed in section V A. Observed vibrational wavenumbers and relative intensities of these new features are listed in Table II.

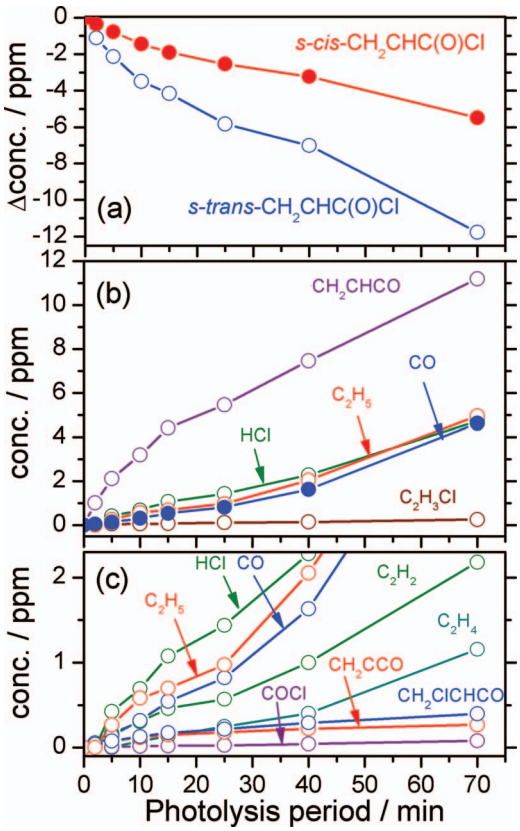

FIG. 3. Mixing ratio profiles as a function of photolysis period at 193 nm for precursors and photolysis products. (a) *s-cis*-$CH_2CHC(O)Cl$ and *s-trans*-$CH_2CHC(O)Cl$; the initial mixing ratios are 78 ± 14 and 150 ± 10 ppm, respectively. (b) $\cdot CH_2CHCO$, C_2H_5, CO, HCl, and C_2H_3Cl. (c) C_2H_2, C_2H_4, $CH_2ClCHCO$, CH_2CCO, and ClCO; initial stages of HCl, C_2H_5, and CO are also shown.

We estimated the changes in mixing ratios of *s-trans*-$CH_2CHC(O)Cl$, *s-cis*-$CH_2CHC(O)Cl$, and $\cdot CH_2CHCO$ after irradiation at 193 nm for 70 min (Fig. 2(b)) to be approximately −(12 ± 2), −(5.5 ± 1.0), and (11 ± 2) ppm, respectively; the errors reflect only standard deviations in fitting. The temporal evolutions in the mixing ratios of these species are shown in Fig. 3. Upon secondary photolysis at 248 nm

TABLE III. Observed wavenumbers and relative IR intensities for lines in various groups ascribable to known species.

Groups	Species	ν/cm^{-1} and relative intensities[a]
A	C_2H_2	3294.9 (14), 3279.6 (41), 733.7 (100)
B	C_2H_4	1440 (16), 948.6 (100)
C	C_2H_5	3124.8 (3.6), 3032.6 (19), 538.5 (100)
D	C_2H_3Cl	1609.5 (100), 943.2 (30), 896.5 (34)
E	$CH_2ClCHCO$	2141.4 (100), 1265.4(7.5), 1019.1 (2.9)
A1	C_2H_2-HCl	3274.2 (183.2), 2784.3/2782.4/2780.6 (273), 1974.2 (27), 748.2 (100)
B1	C_2H_4-HCl	2772.7/2770.5 (415), 964.4 (100)
	CH_3CHCO	2129.2
	CH_2CCO	2122.4

[a]Percentage IR intensities relative to the most intense line of the species are listed in parentheses.

(Fig. 2(c)), the variations in the mixing ratios (ppm) are approximately $\Delta[\cdot CH_2CHCO]:\Delta[C_2H_5]:\Delta[C_2H_4]:\Delta[CO] = -(7.3 \pm 1.0):(5.1 \pm 0.9):(0.56 \pm 0.02):(4.1 \pm 0.8)$.

We observed also weak absorption lines of stable products C_2H_3Cl at 1609.5, 943.2, and 896.5 cm^{-1} (group D),[46] $CH_2ClCHCO$ at 2141.4, 1265.4, and 1019.1 cm^{-1} (group E),[14] C_2H_2-HCl at 3274.2 and 2784.3 cm^{-1} (group A_1),[46] and C_2H_4-HCl at 2772.7 cm^{-1} (group B_1),[27,46] as indicated in Fig. 2 and listed in Table III. Weak lines observed at 2122.4 and 2129.2 cm^{-1} are tentatively assigned to CH_2CCO and CH_3CHCO, respectively; the corresponding lines for these two species isolated in solid Ar are at 2125 (Ref. 47) and 2130 cm^{-1},[48] respectively. Because only the most intense features (C=O stretching mode) of these species were observed, these assignments are tentative. According to Fig. 2(b), we estimated the mixing ratios of C_2H_2, C_2H_4, C_2H_5, C_2H_3Cl, $CH_2ClCHCO$, and CO after photolysis of the matrix at 193 nm for 70 min to be approximately (2.2 ± 0.2), (1.2 ± 0.1), (4.9 ± 0.9), (0.3 ± 0.1), (0.4 ± 0.1), and (4.6 ± 0.7) ppm. The temporal evolution of the mixing ratios of these species as a function of photolysis duration is shown in Fig. 3. Original difference spectra are shown in Fig. S4 of the supplementary material.[42]

Photolysis with light of additional wavelengths was also conducted. When a light-emitting diode (365 nm, 200 mW) was used, we observed no new product. When the light of a medium-pressure mercury lamp filtered to pass the spectral range 313 ± 10 nm was used, only two weak lines at 2103 and 2140 cm^{-1} were observed. We performed photolysis also at 266 nm, but the products were more complicated and the yield of lines in group X ($\cdot CH_2CHCO$) is much smaller. Because the main purpose of this paper is to identify IR spectrum of $\cdot CH_2CHCO$, we discuss only the photolysis experiments of $CH_2CHC(O)Cl$ at 193 nm.

V. DISCUSSION

The UV absorption cross section of $CH_2CHC(O)Cl$ is unreported; we have calculated it to be $\sim 1.5 \times 10^{-20}$ cm^2 $molecule^{-1}$ near 300 nm and $\sim 4 \times 10^{-17}$ cm^2 $molecule^{-1}$ near 200 nm using time-dependent density-functional theory (TD-DFT). The *s-trans* → *s-cis* isomerization of $CH_2CHC(O)Cl$ was reported to occur upon photolysis with wavelength greater than 310 nm.[14] We also observed such conversion upon irradiation of the matrix sample at 295 nm, but we were unable to convert all *s-trans*-$CH_2CHC(O)Cl$ to *s-cis*-$CH_2CHC(O)Cl$ after irradiation for 2 h.

According to Szpunar *et al.*, the major channel upon photolysis of $CH_2CHC(O)Cl$ in a molecular beam at 193 nm is the fission of the C−Cl bond; all C_2H_3CO radicals thus produced have enough internal energy to undergo subsequent dissociation to form $CH_2CH + CO$.[15] A minor channel for formation of $HCl + CH_2CCO$ was also observed, and all CH_2CCO (propadienone) underwent secondary dissociation to form $CH_2C: + CO$. Because energy quenching is expected to be efficient in solid *p*-H_2, the primary products C_2H_3CO and CH_2CCO might be stabilized under our experimental conditions; hence CH_2CCO and three possible conformers, *s-cis*-$CH_2C\dot{H}CO$, *s-trans*-$CH_2C\dot{H}CO$, and $\cdot CH_2CHCO$, of C_2H_3CO are the possible carriers of the newly observed lines in group X.

A. Assignment of lines in group X to the 3-propenonyl ($\cdot CH_2CHCO$) radical

Baskir and Nefedov reported infrared spectra of *s-cis* and *s-trans*-$CH_2C\dot{H}CO$ radicals obtained after UV ($\lambda > 248$ nm) photolysis of $H_2C = CHCH_2OO$ in an Ar matrix.[22] They reported characteristic intense lines at 1832.0 and 1823.1 cm^{-1} for the CO stretching mode of *s-cis*- and *s-trans*-$CH_2C\dot{H}CO$, respectively, with the latter being more intense; additional weak lines at 1094.4, 975.3, and 870.7 cm^{-1} were also assigned to $CH_2C\dot{H}CO$. There is no report of an IR spectrum of the $\cdot CH_2CHCO$ radical. Chapman *et al.* reported IR spectrum of propadienone (CH_2CCO) in Ar or N_2 matrices; CH_2CCO was prepared by pyrolysis of gaseous 3-diazo-2,4(5H)-furadione.[47] The most intense line observed at 2125 cm^{-1} corresponds to the C=C=O antisymmetric stretching mode; other reported lines are listed in Table II.

The intensities of absorption lines in group X, listed as relative values in Table II, increased rapidly during irradiation in the first 15 min and increased less rapidly afterwards; those of other lines are smaller than 7% of the most intense one at 2103.1 cm^{-1}. Upon secondary photolysis at 248 nm, the intensities of these lines in group X decreased whereas those of lines of C_2H_5, C_2H_4, and CO increased.

No reported species has a spectral pattern similar to that observed for lines in group X. We observed a characteristically intense line near 2103.1 cm^{-1} in group X, but no significant absorption near the 1830 cm^{-1} region. The wavenumber of this line is near that of the line at 2125 cm^{-1} of CH_2CCO, but other reported lines of CH_2CCO (Table II) do not match with other lines in group X.[47] Furthermore, a line observed at 2122.4 cm^{-1} (Fig. 2(b)) is near the line at 2125 cm^{-1} reported for CH_2CCO isolated in solid Ar. We observed also a weak IR absorption feature of CH_3CHCO at 2129.2 cm^{-1}, of which the intensity increased significantly upon IR irradiation of the193-nm-irradiated matrix; the corresponding line was reported to be 2130 cm^{-1} in an Ar matrix.[48] Another weak line observed at 2141.4 cm^{-1} is assigned to $CH_2ClCHCO$; the corresponding value is reported as (2143.6−2138.0) cm^{-1} in an Ar matrix.[14] The wavenumber of the observed intense line at 2103.1 cm^{-1} that is slightly smaller than those of ketene (2142.0 cm^{-1}),[49] $CH_2ClCHCO$ (2141.4 cm^{-1}), CH_2CCO (2125 cm^{-1}), and CH_3CHCO (2129.2 cm^{-1}) but greater than those of *s-cis*- and *s-trans*-$CH_2C\dot{H}CO$ indicates that the most likely carrier of this line in group X is $\cdot CH_2CHCO$; this observation is consistent with the calculated bond length of 1.169 Å for CO in $\cdot CH_2CHCO$, slightly greater than 1.164 Å in $CH_2ClCHCO$ but much smaller than corresponding values 1.188/1.190 Å in *s-cis*/*s-trans*-$CH_2C\dot{H}CO$.

In Fig. 4(a) we inverted the difference spectrum obtained upon secondary photolysis at 248 nm for 10 min (Fig. 2(c)) so that lines in group X are pointing upward; the negative lines are truncated and regions due to interference by absorption of $CH_2CHC(O)Cl$ and secondary products are marked with grey. In Figs. 4(b)–4(f) we plot IR spectra of $\cdot CH_2CHCO$, $CH_2ClCHCO$, CH_2CCO, *s-cis*-$CH_2C\dot{H}CO$, and

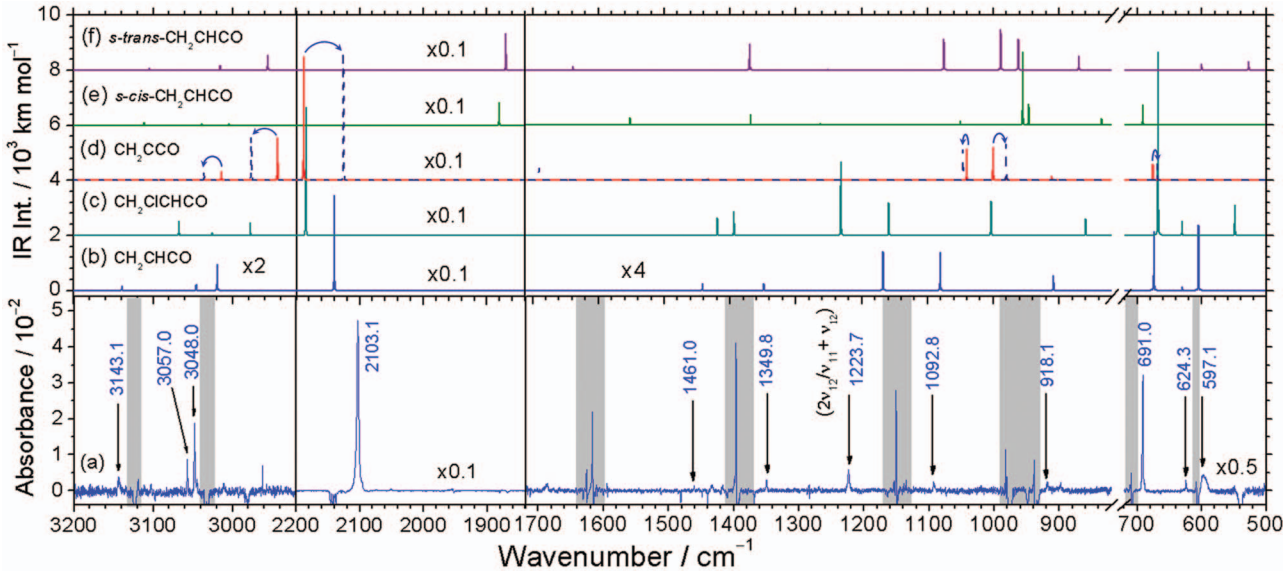

FIG. 4. Comparison of experimental spectrum with those simulated for possible candidates. (a) Inverted spectrum of Fig. 2(c), obtained upon secondary photolysis of the 193-nm-irradiated matrix of $CH_2CHC(O)Cl/p\text{-}H_2$ (1/3000) at 248 nm for 10 min. IR spectra simulated according to anharmonic vibrational wavenumbers and IR intensities of $\cdot CH_2CHCO$ (b), $CH_2ClCHCO$ (c), CH_2CCO (d), *s-cis*-$CH_2C\dot{H}CO$ (e), and *s-trans*-$CH_2C\dot{H}CO$ (f) predicted with the B3PW91/aug-cc-pVDZ method. The lines in group X, assigned to the 3-propenonyl ($\cdot CH_2CHCO$) radical, are marked with wavenumbers in trace (a). Experimental values of CH_2CCO (Ref. 47) are shown as dotted lines in trace (d). Regions due to interference by absorption of $CH_2CHC(O)Cl$ and secondary products are marked with grey.

s-trans-$CH_2C\dot{H}CO$ radicals, respectively, simulated according to the anharmonic vibrational wavenumbers and IR intensities predicted with the B3PW91/aug-cc-pVDZ method and a spectral width of 0.25 cm^{-1}. For CH_2CCO, the experimental values are plotted as blue dotted lines in trace (d) for comparison with predicted values; the shifts are marked with arrows. As discussed previously, the most intense line observed at 2103.1 cm^{-1} is characteristic of the C=C=O antisymmetric stretching mode of species with a C=C=O moiety; the spectral patterns of *s-cis*-$CH_2C\dot{H}CO$ and *s-trans*-$CH_2C\dot{H}CO$ (Figs. 4(e) and 4(f)) disagree with that observed for group X.

The observed wavenumbers and relative IR intensities of lines in group X agree satisfactorily with those predicted for $\cdot CH_2CHCO$ radical (Fig. 4(b)), but neither $CH_2ClCHCO$ nor CH_2CCO (Figs. 4(c) and 4(d)), as shown in the figures and listed in Table II. The most intense feature at 2103.1 cm^{-1} agrees better with the value 2139 cm^{-1} predicted for the C=C=O antisymmetric stretching (ν_4) mode of $\cdot CH_2CHCO$ than that of the C=O stretching mode at 2184 cm^{-1} for $CH_2ClCHCO$ and 2187 cm^{-1} for CH_2=CCO; the experimental value is 2125 cm^{-1} for the latter.[47] Other significant features at 3048.0, 691.0, and 597.1 cm^{-1} agree satisfactorily with values 3019 (ν_3, CH stretching mode), 674 (ν_{10}, CH out-of-plane bending mode), and 605 cm^{-1} (ν_{12}, CH_2 wagging mode), respectively, predicted for $\cdot CH_2CHCO$. Eight additional weak lines also agree with those predicted for $\cdot CH_2CHCO$, as compared in Table II and Fig. 4. The average deviation between observed and predicted anharmonic vibrational wavenumbers is 14 ± 10 cm^{-1}, with the largest deviation ~30 cm^{-1} for the ν_4 mode.

The weak line at 1223.7 cm^{-1} observed in group X corresponds to no predicted fundamental vibrational wavenumber of $\cdot CH_2CHCO$. Tentatively, the line observed at 1223.7 cm^{-1} is assigned to the combination modes ($\nu_{11} + \nu_{12}$) and/or $2\nu_{12}$; the predicted values are 1236 cm^{-1} for $\nu_{11} + \nu_{12}$ and 1235 cm^{-1} for $2\nu_{12}$.

After considering the observed photolytic behavior upon primary and secondary photolysis of a $CH_2CHC(O)Cl/p\text{-}H_2$ (1/3000) matrix at 3.2 K and the agreement in vibrational wavenumbers and relative IR intensities between lines in groups X and those predicted quantum-chemically, we assigned these new features in group X to IR absorption of the 3-propenonyl ($\cdot CH_2CHCO$) radical.

B. Photolytic mechanism of $CH_2CHC(O)Cl$ in solid *p*-H_2

The enthalpies of reaction for the fission of the C−Cl bond of $CH_2CHC(O)Cl$ was calculated to be 348 and 342 kJ mol^{-1} for formation of *s-cis*-$CH_2C\dot{H}CO$ and *s-trans*-$CH_2C\dot{H}CO$ conformers, respectively, with the G3//B3LYP method.[15] The C−Cl bond fission of $CH_2CHC(O)Cl$ is known to occur on the singlet S_1 surface;[13,20] the $S_1 \leftarrow S_0$ transition origin was calculated to be 353 and 457 kJ mol^{-1} according to the MRCI//CASSCF/cc-pVDZ and the MP2/6-31G* methods, respectively.[20,14] Five primary dissociation channels are possible:

$$CH_2CHC(O)Cl \rightarrow C_2H_3CO + Cl, \quad (1)$$

$$\rightarrow CH_2CCO + HCl, \quad (2)$$

$$\rightarrow C_2H_3 + ClCO, \quad (3)$$

$$\rightarrow C_2H_3Cl + CO, \quad (4)$$

$$\rightarrow CH_2ClCHCO. \quad (5)$$

Reaction (2) is associated with a four-center elimination, whereas reaction (5) is associated with a 1,3-Cl migration.

The molecular-beam experiments indicate that, upon irradiation of $CH_2CHC(O)Cl$ at 193 nm (619 kJ mol^{-1}), two C−Cl fission channels and one HCl-elimination channel occur. In CH_3CN solution, upon irradiation of $CH_2CHC(O)Cl$ at 193 and 266 nm, the reaction proceeds via nonadiabatic paths $S_1 \rightarrow T_1 \rightarrow S_0$ and the 1,3-Cl migration proceeds via a stepwise mechanism involving radical dissociation followed by recombination to form $CH_2ClCHCO$. In an Ar matrix, irradiation of $CH_2CHC(O)Cl$ with light of $\lambda \geq 310$ nm yields $CH_2ClCHCO$. In this work, irradiation at 193 nm of $CH_2CHC(O)Cl$ isolated in solid *p*-H_2 yielded $\cdot CH_2CHCO$ as a major product. We performed irradiation with light also of $\lambda \geq 310$ nm and observed only one weak line of $\cdot CH_2CHCO$ at 2103 cm^{-1} and another one at 2141 cm^{-1} that is tentatively assigned to $CH_2ClCHCO$. Observation of $\cdot CH_2CHCO$ in *p*-H_2 indicates that the matrix cage effect is indeed diminished.

To derive a photolysis mechanism based on results of continuous photolysis experiments in a solid matrix is difficult because the matrix cage effect and secondary photolysis might play important roles to obscure the results from the primary processes. To examine the temporal evolution of all photodissociation products, we plot in Fig. 3 the mixing ratios (in ppm) of products $\cdot CH_2CHCO$, C_2H_2, C_2H_4, C_2H_5, C_2H_3Cl, $CH_2ClCHCO$, CH_2CCO, CO, ClCO, and HCl, along with the decay of precursors *s-cis*-$CH_2CHC(O)Cl$ and *s-trans*-$CH_2CHC(O)Cl$, as a function of duration of photolysis. The mixing ratios derived for $\cdot CH_2CHCO$, C_2H_5, $CH_2ClCHCO$, CH_2CCO, ClCO, and C_2H_3Cl according to quantum-chemically predicted IR intensities might have error as large as a factor of two. Although Cl atom can be probed with the line at 943.7 cm^{-1} associated with its weak spin-orbit transition $^2P_{1/2} \leftarrow {}^2P_{3/2}$ reported by Raston and Anderson,[50] we observed an insignificant absorption feature of Cl at 943.7 cm^{-1} due to its small concentration; an upper limit of the mixing ratio of Cl atom was estimated to be 230 ppm when a maximum of integrated absorbance of 0.005 cm^{-1} and the gas-phase transition strength of 9.45×10^{-26} km $molecule^{-1}$ was used.[50] This spin-orbit transition of Cl is too weak to be a suitable probe of Cl atoms produced in our experiments.

To estimate the branching ratios among channels (1)–(5), we should consider the mixing ratios of the primary products that undergo negligible secondary reactions and also cannot be produced via secondary reactions. Our best choices are $\cdot CH_2CHCO$, CH_2CCO, ClCO, and $CH_2ClCHCO$ for channels (1)–(3) and (5); for channel (4), because C_2H_3Cl dissociates readily at 193 nm and because CO might be produced from other secondary processes, we used CO to derive the upper limit. Because $\cdot CH_2CHCO$, CH_2CCO, ClCO, and $CH_2ClCHCO$ might also undergo secondary photolysis, the corresponding values should be taken as lower limits. As calculated IR intensities might have large errors, the branching ratios estimated here might also have errors as large as a factor of 2. After irradiation with light at 193 nm for 15 min, we estimated the mixing ratios of $\cdot CH_2CHCO$, CH_2CCO, ClCO, CO, and $CH_2ClCHCO$ to be approximately (4.4 ± 0.4), (0.15 ± 0.02), (0.02 ± 0.01), (0.54 ± 0.08), and (0.17 ± 0.03) ppm, with a branching ratio (0.83 ± 0.07):(0.03 ± 0.01):(0.004 ± 0.002):<(0.10 ± 0.02):(0.03 ± 0.01) for channels (1)–(5); the errors reflect only the standard deviations of the fitting among several lines of each species. The detailed mechanism for formation of secondary products and the estimation of branching ratios are presented in the supplementary material.[42]

Perhaps the most significant result from the estimation of branching ratios is that channel (1) is dominant upon photodissociation at 193 nm, and other channels likely have branching ratios less than 10%. Although Szpunar *et al*. estimated the branching ratio of channels (1) to (2) to be ∼3–1 when $CH_2CHC(O)Cl$ in a molecular beam was irradiated at 193 nm,[15] they reported that it was only a rough estimate because of possible errors. Szpunar *et al*. could not identify the conformation of C_2H_3CO; the two distributions of translational energy for the C−Cl fission processes were attributed to dissociation along the electronically excited surface and the ground surface. In this work we observed IR absorption of the $\cdot CH_2CHCO$ radical, whereas absorption of neither *s-cis*-$CH_2\dot{C}HCO$ nor *s-trans*-$CH_2\dot{C}HCO$ was identified. This condition is consistent with the quantum-chemical calculations that predict the most stable isomer to be $\cdot CH_2CHCO$ and the barriers for conversion from $CH_2\dot{C}HCO$ to $\cdot CH_2CHCO$ to be small, <11 kJ mol^{-1}.

The observation of no absorption of $\cdot CH_2CHCO$ but only lines of $CH_2\dot{C}HCO$ isolated in solid Ar at 1823.1 and 1832.0 cm^{-1} and several weak ones at 1094.4, 975.3, and 870.7 cm^{-1} by Baskir and Nefedov is not inconsistent with our observation, because these features were observed upon photolysis of allylperoxy, $H_2C{=}CHCH_2OO$,[22] not from $CH_2CHC(O)Cl$. Furthermore, their reported vibrational wavenumbers agree unsatisfactorily with theoretical calculations listed in Table II. To decipher these discrepancies, similar experiments capable of observation of more lines are desirable. The observation of only 3-chloro-1,2-propenone, $CH_2ClCHCO$, with a characteristic broad feature near 2139 cm^{-1} by Pietri *et al*. upon photolysis of $CH_2CHC(O)Cl$ isolated in an Ar matrix at 10 K with light ≥310 nm from a high-pressure Hg lamp might be due to secondary reaction of Cl + C_2H_3CO because of the cage effect.[14] Our observation of $\cdot CH_2CHCO$ rather than $CH_2ClCHCO$ demonstrates again the advantage of a diminished cage effect of *p*-H_2 to produce free radicals via photolysis *in situ*.

VI. CONCLUSION

Photodissociation at 193 nm of $CH_2CHC(O)Cl$ isolated in solid *p*-H_2 has been investigated using IR absorption spectroscopy. IR lines of the 3-propenonyl ($\cdot CH_2CHCO$) radical were identified with a characteristic intense feature at 2103.1 cm^{-1} (C=C=O antisymmetric stretch) and 11 weaker features including more significant ones at 3048.0 (ν_3, CH stretch), 691.0 (ν_{10}, CH out-of-plane bend), and 597.1 cm^{-1} (ν_{12}, CH_2 wag). The experimentally observed fundamental line positions are new and their wavenumbers and relative IR intensities agree satisfactorily with those predicted with the B3PW91/aug-cc-pVDZ method for $\cdot CH_2CHCO$. Our observation of the $\cdot CH_2CHCO$ radical rather than $CH_2\dot{C}HCO$ is consistent with theoretical predictions indicating

that ·CH_2CHCO is the most stable isomer and that the isomerization barrier from $CH_2C\dot{H}CO$ to ·CH_2CHCO is small. The observation of ·CH_2CHCO from photolysis of $CH_2CHC(O)Cl$ rather than $CH_2ClCHCO$ reported for photolysis of $CH_2CHC(O)Cl$ in solid Ar clearly illustrates that solid *p*-H_2 has a diminished cage effect, so that the Cl atom might escape from the original cage and ·CH_2CHCO becomes isolated.

ACKNOWLEDGMENTS

National Science Council of Taiwan (Grant No. NSC102-2745-M009-001-ASP) and the Ministry of Education, Taiwan ("Aim for the Top University Plan" of National Chiao Tung University) supported this work. The National Center for High-performance Computing provided computer time.

[1]Y. S. Yang, G. R. Qi, J. W. Qian, and S. L. Yang, J. Appl. Polym. Sci. **68**, 665 (1998).
[2]L. Ferrie, S. Bouzbouz, and J. Cossy, Org. Lett. **11**, 5446 (2009).
[3]H. M. Wortelboer, M. Usta, J. J. Zanden, P. J. Bladeren, I. M. C. M. Rietjens, and N. H. P. Cnubben, Biochem. Pharmacol. **69**, 1879 (2005).
[4]T. Billard, Chem. Eur. J **12**, 974 (2006).
[5]H. Lee, M. J. Nam, and J. H. Choi, J. Chem. Phys. **124**, 044311 (2006).
[6]J. E. Katon and W. R. Feairheller, Jr., J. Chem. Phys. **47**, 1248 (1967).
[7]R. L. Redington and J. R. Kennedy, Spectrochim. Acta A **30**, 2197 (1974).
[8]K. Hagen and K. Hedberg, J. Am. Chem. Soc. **106**, 6150 (1984).
[9]J. R. Durig, R. J. Berry, and P. Groner, J. Chem. Phys. **87**, 6303 (1987).
[10]J. R. Durig, Y. Li, and Y. Jin, Chem. Phys. **213**, 181 (1996).
[11]L. A. Koroleva, V. I. Tyulin, V. K. Matveev, and Y. A. Pentin, Russ. J. Phys. Chem. A **85**, 433 (2011).
[12]G. R. Allen and D. K. Russell, New J. Chem. **28**, 1107 (2004).
[13]M. F. Arendt, P. W. Browing, and L. J. Butler, J. Chem. Phys. **103**, 5877 (1995).
[14]N. Pietri, M. Monnier, and J.-P. Aycard, J. Org. Chem. **63**, 2462 (1998).
[15]D. E. Szpunar, J. L. Miller, L. J. Butler, and F. Qi, J. Chem. Phys. **120**, 4223 (2004).
[16]K.-C. Lau, Y. Liu, and L. J. Butler, J. Chem. Phys. **123**, 054322 (2005).
[17]W. Wu, K. Liu, C. Yang, H. Zhao, H. Wang, Y. Yu, and H. Su, J. Phys. Chem. A **113**, 13892 (2009).
[18]Y. C. Fan, W. W. Qiang, L. K. Hui, W. Huan, and S. H. Mei, Sci. China Chem. **55**, 359 (2012).
[19]M. Ge, C. Ma, and W. Xue, J. Phys. Chem. A **113**, 3108 (2009).
[20]G.-L. Cui, Q.-S. Li, F. Zhang, W.-H. Fang, and J.-G. Yu, J. Phys. Chem. A **110**, 11839 (2006).
[21]A. L. Cooksy, J. Phys. Chem. A **102**, 5093 (1998).
[22]E. G. Baskir and O. M. Nefedov, Russ. Chem. Bull. **45**, 99 (1996).
[23]N. Sogoshi, T. Wakabayashi, T. Momose, and T. Shida, J. Phys. Chem. A **101**, 522 (1997).
[24]M. Bahou and Y.-P. Lee, J. Chem. Phys. **133**, 164316 (2010).
[25]Y.-F. Lee, L.-J. Kong, and Y.-P. Lee, J. Chem. Phys. **136**, 124510 (2012).
[26]Y.-F. Lee and Y.-P. Lee, J. Chem. Phys. **134**, 124314 (2011).
[27]J. C. Amicangelo, B. Golec, M. Bahou, and Y.-P. Lee, Phys. Chem. Chem. Phys. **14**, 1014 (2012).
[28]M. Bahou, J.-Y. Wu, K. Tanaka, and Y.-P. Lee, J. Chem. Phys. **137**, 084310 (2012).
[29]M. Bahou, H. Witek, and Y.-P. Lee, J. Chem. Phys. **138**, 074310 (2013).
[30]P. Das, M. Bahou, and Y.-P. Lee, J. Chem. Phys. **138**, 054307 (2013).
[31]P. L. Raston and D. T. Anderson, Phys. Chem. Chem. Phys. **8**, 3124 (2006).
[32]M. Ruzi and D. T. Anderson, J. Chem. Phys. **137**, 194313 (2012).
[33]S. Tam and M. E. Fajardo, Appl. Spectrosc. **55**, 1634 (2001).
[34]I. F. Silvera, Rev. Mod. Phys. **52**, 393 (1980).
[35]P. Jona, M. Gussoni, and G. Zerbi, J. Phys. Chem. **85**, 2210 (1981).
[36]G. B. Lebron and T. L. Tan, Int. J. Spectrosc. **2012**, 1 (2012).
[37]W. S. Benedict, R. Herman, G. E. Moore, and S. Silverman, J. Chem. Phys. **26**, 1671 (1957).
[38]A. D. Becke, J. Chem. Phys. **98**, 5648 (1993).
[39]J. P. Perdew, K. Burke, and Y. Wang, Phys. Rev. B **54**, 16533 (1996).
[40]T. H. Dunning, Jr., J. Chem. Phys. **90**, 1007 (1989).
[41]M. J. Frisch, G. W. Trucks, H. B. Schlegel *et al*., GAUSSIAN 09, Revision A02, Gaussian, Inc., Wallingford, CT, 2009.
[42]See supplementary material at http://dx.doi.org/10.1063/1.4818880 for optimized geometries of s-*cis*/s-*trans* $CH_2CHC(O)Cl$, $CH_2ClCHCO$, and CH_2CCO, harmonic and anharmonic vibrational wavenumbers and IR intensities of *s-cis*-/*s-trans*-$CH_2CHCOCl$ calculated with the B3PW91/aug-cc-pVDZ method, difference spectra of the $CH_2CHC(O)Cl$/*p*-H_2 matrix upon 295 nm irradiation to distinguish the two isomers, difference spectra of $CH_2CHC(O)Cl$/*p*-H_2 matrix at 3.2 K upon photolysis at 193 nm for 2–70 min, and detailed discussion for determination of branching ratios.
[43]R. D. Brown, P. D. Godfrey, R. Champion, and D. McNaughton, J. Am. Chem. Soc. **103**, 5711 (1981).
[44]R. D. Brown, R. Champion, P. S. Elmes, and P. D. Godfrey, J. Am. Chem. Soc. **107**, 4109 (1985).
[45]S. Tam and M. E. Fajardo, J. Low Temp. Phys. **122**, 345 (2001).
[46]B. Golec and Y.-P. Lee, J. Chem. Phys. **135**, 174302 (2011).
[47]O. L. Chapman, M. D. Miller, and S. M. Pitzenberger, J. Am. Chem. Soc. **109**, 6867 (1987).
[48]P. R. Winter, B. Rowland, W. P. Hess, J. G. Radziszewski, M. R. Nimlos, and G. B. Ellison, J. Phys. Chem. A **102**, 3238 (1998).
[49]C. B. Moore and G. C. Pimentel, J. Chem. Phys. **38**, 2816 (1963).
[50]P. L. Raston and D. T. Anderson, J. Chem. Phys. **126**, 021106 (2007).